**OPEN**

Correspondence and
requests for materials
should be addressed to
L.S. (song2012@ustc.
edu.cn) or S.S.X.
(ssxie@iphy.ac.cn)

# Super-stretchable, Transparent Carbon Nanotube-Based Capacitive Strain Sensors for Human Motion Detection

Le Cai[1,2], Li Song[3], Pingshan Luan[1,2], Qiang Zhang[1,2], Nan Zhang[1,2], Qingqing Gao[1,2], Duan Zhao[1,2], Xiao Zhang[1,2], Min Tu[1,2], Feng Yang[1,2], Wenbin Zhou[1,2], Qingxia Fan[1,2], Jun Luo[1], Weiya Zhou[1], Pulickel M. Ajayan[4] & Sishen Xie[1,5]

[1]Beijing National Laboratory for Condensed Matter Physics, Institute of Physics, Chinese Academy of Sciences, Beijing 100190, China, [2]Graduate School of the Chinese Academy of Sciences, Beijing 100049, China, [3]National Synchrotron Radiation Laboratory, University of Science and Technology of China, Hefei 230029, China, [4]Department of Mechanical Engineering and Materials Science, Rice University, Houston, TX77005, USA, [5]Key Laboratory for the Physics and Chemistry of Nanodevices, Department of Electronics, Peking University, Beijing, 100871, China.

Realization of advanced bio-interactive electronic devices requires mechanically compliant sensors with the ability to detect extremely large strain. Here, we design a new multifunctional carbon nanotube (CNT) based capacitive strain sensors which can detect strains up to 300% with excellent durability even after thousands of cycles. The CNT-based strain gauge devices exhibit deterministic and linear capacitive response throughout the whole strain range with a gauge factor very close to the predicted value (strictly 1), representing the highest sensitivity value. The strain tests reveal the presented strain gauge with excellent dynamic sensing ability without overshoot or relaxation, and ultrafast response at sub-second scale. Coupling these superior sensing capabilities to the high transparency, physical robustness and flexibility, we believe the designed stretchable multifunctional CNT-based strain gauge may have various potential applications in human friendly and wearable smart electronics, subsequently demonstrated by our prototypical data glove and respiration monitor.

R ecent developments in flexible and stretchable electronics, either through structural consideration or by exploring novel materials[1,2], have imparted otherwise rigid and brittle electronic devices mechanical compliance and bio-compatibility, paving the way for energy-efficient, lightweight, portable, wearable and even implantable electronics[3]. Examples include stretchable and large area display that can undergo complex deformations[4], bio-inspired material and structural designs that enable bionic functions[5], and printable sensory system capable of detecting planar strains, normal pressure, temperature, light, moisture and chemical/biological species[6]. Multifunctional sensors, in particular, with sensing abilities akin to or beyond those of human skin[6–12], are essential for applications such as interactive electronics[13], structural health monitoring[14], smart clothing[15], robotic systems with advanced sensing capabilities[16], human motion detection[8] and so on. Among the various types of sensors, strain gauge is one of the most important smart sensors, which have been widely used in the measurements of strain, acceleration and tension, as well as structural health monitoring. Conventional strain gauges, made of metal foils, register resistance changes under tensile strains. Actually, mechanical compliance and large strain range ($\gg$5%), obviously not the case of metal foils, are required to meet the demands of wearable electronics[15], human motion detection[8] and interactive robots[17]. Although mercury-in-rubber strain gauge has been used in the biological measurements for decades[18], the maximum strain limit and toxicity of mercury still block their practically wide applications. In addition, the combination of conformability and optical transparency will facilitate intelligent electronics and self-powered robot where strain sensors are integrated with optoelectronic devices and direct observation through the devices is necessary[3]. Therefore, stretchability and transparency have to be incorporated into strain gauges for many specific applications.

It is well known that the integration of stretchability into any electronic device relies on the realization of stretchable conductors that maintain stable and reliable electrical conductance under large strains ($\gg$1%)[3]. Traditionally, special designs in structures and configurations are adopted to obtain stretchability[1]. For instance, wavy structured ultrathin metal ribbons can withstand strains up to 100% by a mechanism where planar strains

are absorbed by the nonplanar movements of the arch-shaped parts while the metal ribbons themselves are subjected to minimum harmful strains[19]. An alternative approach to stretchability is to explore novel materials that are intrinsically stretchable[2]. For decades, people have been using conductive rubber based on elastomer loaded with carbon black. Their resistivity and strain dependence, however, are too large to be useful in stretchable electronics. Recent investigations suggested that acceptable performance could be obtained by replacing carbon black with more conductive and structurally favorable materials, e.g. carbon nantoubes[4,20,21], graphene[22], ultrathin metal films deposited on elastomer substrate[23] and metal nanoparticles dispersed in elastomer matrix[23,24].

Carbon nanotubes (CNTs) are nanometer sized fibers with extremely high aspect ratio ($>10^6$), Young's modulus ($\sim 1$ TPa) and tensile strength ($\sim 100$ GPa), current carrying ability ($10^9$ A/cm$^2$), and thermal conductivity (3500 W/mK)[25]. By virtue of the small sizes and ultimate fibril structures, macro-assemblies of CNTs take diverse organizing forms[26], providing plenty of opportunities for the realization of various CNT-based functional materials and devices[27–29]. Particularly, the intertwining and curvilinear attributes of the CNTs make them intrinsically stretchable and suitable for the fabrication of stretchable devices. In addition, ultrathin CNT films have shown excellent transparent-conductive performance and are most competitive candidates for the fabrication of highly transparent and stretchable electrodes[7,30,31]. Reported examples include stretchable interconnects and electrodes based on ultrathin films and vertical aligned forests of CNTs embedded in elastomers[30,32–35], as well as super-growth CNTs dispersed in elastomer matrix[4,20]. Furthermore, several CNT-based stretchable electronic and optoelectronic devices-organic light-emitting diodes (OLEDs)[36], super capacitors[37], large area displays[4], thermoacoustic loudspeakers[38], and field effect emitting device[39], to name a few-have also been demonstrated.

In the particular case of strain gauges, the realization of stretchability requires not only stretchable conductance but also recoverable and stable, often resistive or capacitive, responses to large strains. Both resistive and capacitive stretchable strain gauges that could detect strains up to 100% have been demonstrated based on carbon nanotubes[8,17]. However, fabricating stretchable strain gauges with high sensitivity, optical transparency, durability and stability in a simple and large-scale manner still challenges the scientific and engineering communities. Here we design a new multifunctional CNT-based capacitive stretchable strain gauges that can measure strains as large as 300%, with high sensitivity (close to 1), excellent durability (10000 cycles at 100% strains), fast response (delay time well below 100 ms), high optical transparency (nearly80% at 550 nm), excellent stability and no hysteresis or relaxation.

## Results

**Operating principle and fabrication of CNT-based transparent capacitive strain gauges.** To create the strain gauges, two layers of CNT films, acting as electrodes, were laid on the two sides of a lamina of silicone elastomer to form a parallel plate-like capacitor. The fabrication procedures are schematically shown in Fig. 1a and details can be found in Methods section. When the sample is stretched, the changes in strain manifest themselves as changes in capacitance. As a result of uniaxial stretching, the sizes of the sample change, in particular: its length increases while its width and thickness decrease, due to the famous Poisson effect, which will lead to a rise in the total capacitance (as illustrated in Fig. 1b). Assuming the silicone elastomer film was isotropic and incompressible, the sizes of the deformed sample can be expressed as

$$l = \lambda \bullet l_0 \qquad w = 1 \Big/ \sqrt{\lambda} \bullet w_0$$

$$t = 1 \Big/ \sqrt{\lambda} \bullet t_0 \quad \lambda = 1 + \varepsilon$$

where $l_0$, $w_0$ and $t_0$ denote the length, width and thickness of the device in its natural state, and $\varepsilon$ is the applied strain. Then, according to the ideal parallel-plate model and providing the CNT films follow the same Poisson deformation with the silicone elastomer, the capacitance of the stretched device is

$$C = \varepsilon_0 \varepsilon_r \frac{l \bullet w}{t} = \varepsilon_0 \varepsilon_r \frac{\lambda \bullet l_0 \bullet 1 \Big/ \sqrt{\lambda} \bullet w_0}{1 \Big/ \sqrt{\lambda} \bullet t_0} = \varepsilon_0 \varepsilon_r \frac{\lambda \bullet l_0 \bullet w_0}{t_0} = \lambda \bullet C_0$$

$$C_0 = \varepsilon_0 \varepsilon_r \frac{l_0 \bullet w_0}{t_0}$$

where $C_0$ denotes the initial capacitance, $\varepsilon_0$ and $\varepsilon_r$ represent the permittivity of vacuum and the relative permittivity of silicone, respectively. Consequently, the simple parallel-plate model predicts a linear capacitive response to the applied strain, providing that the overlap between the opposing CNT films is stable. In addition, the capacitive gauge factor, defined as $(\Delta C/C_0)/\varepsilon$, equals to 1.

We want to note here that the fringing effect should be taken into account for capacitors with finite-size electrodes. According to Palmer's calculations[40], the exact value of the length-normalized capacitance of a parallel plate capacitor is determined by the ratio of w/t, where w and t represent the width of the electrodes and the separation distance between them, respectively. In the case of Poisson capacitive strain gauge discussed here, the electrodes width and separation distance change synchronous when stretched so that the w/t ratio, thus the length-normalized capacitance remains constant. That means, Palmer's model should predict the same linear response with the simple ideal parallel-plate model.

Carbon nanotube films, mainly consisting of single and double walled nanotubes, were synthesized continuously from a floating catalyst chemical vapor deposition (FCCVD) furnace[41]. The sheet conductance and optical transparency of the films could be controlled by adjusting the growth conditions. The films were composed of random networks of CNT bundles with diameter of about 20 nm, as shown in Fig. 2a,b. Despite that CNT films with extremely high transmittance (as high as 95% at 550 nm) could be obtained, they were not suitable for the Poisson capacitive strain sensors because of the existence of micrometer-sized voids, as shown in Fig. 2a. These voids might lead to unpredictable capacitive responses due to the unstable overlap between the opposing CNT films. Besides, the large value and standard deviation of resistance (Fig. 2c) of such films might lead to unreliable strain gauging performance of the final device. The compromise between the transparency and nanotube coverage should thus be a careful consideration in the preparation procedure of the CNT-based strain gauges. In order to obtain optimum stretchability, transparency and stability, we chose CNT films with a transmittance of 90% at 550 nm. Microscopic morphology characterizations (Fig. 2b) confirmed that such films possessed full areal coverage, ensuring stable overlap between the opposing electrodes and reliable sensing performances of the resulting strain gauges. In addition, their sheet conductance (Fig. 2c) is sufficient for the transparent capacitive strain gauges.

Figure 1c shows the digital image of two as-prepared transparent capacitive strain gauges, manifesting their optical transparency. As shown in Fig. 1d, thanks to the noninvasiveness of the fabrication method and the optical transparency of silicone elastomers[30], the strain gauge devices retained the high transmittance of the original CNT films, which has not been reported in literature. Two kinds of silicone rubber were used, namely Dow Corning Sylgard 184 (noted as PDMS) and Smooth-on Dragon skin 30 (noted as Dragon skin). The maximum strain that PDMS elastomer can sustain is 160%, limiting the large strain performance of the resulting strain gauges which usually break at strains around 130%. For the strain gauges subjected to strains larger than 150%, Dragon skin (elongation, 364%) was selected. Even though Dragon skin is described to be
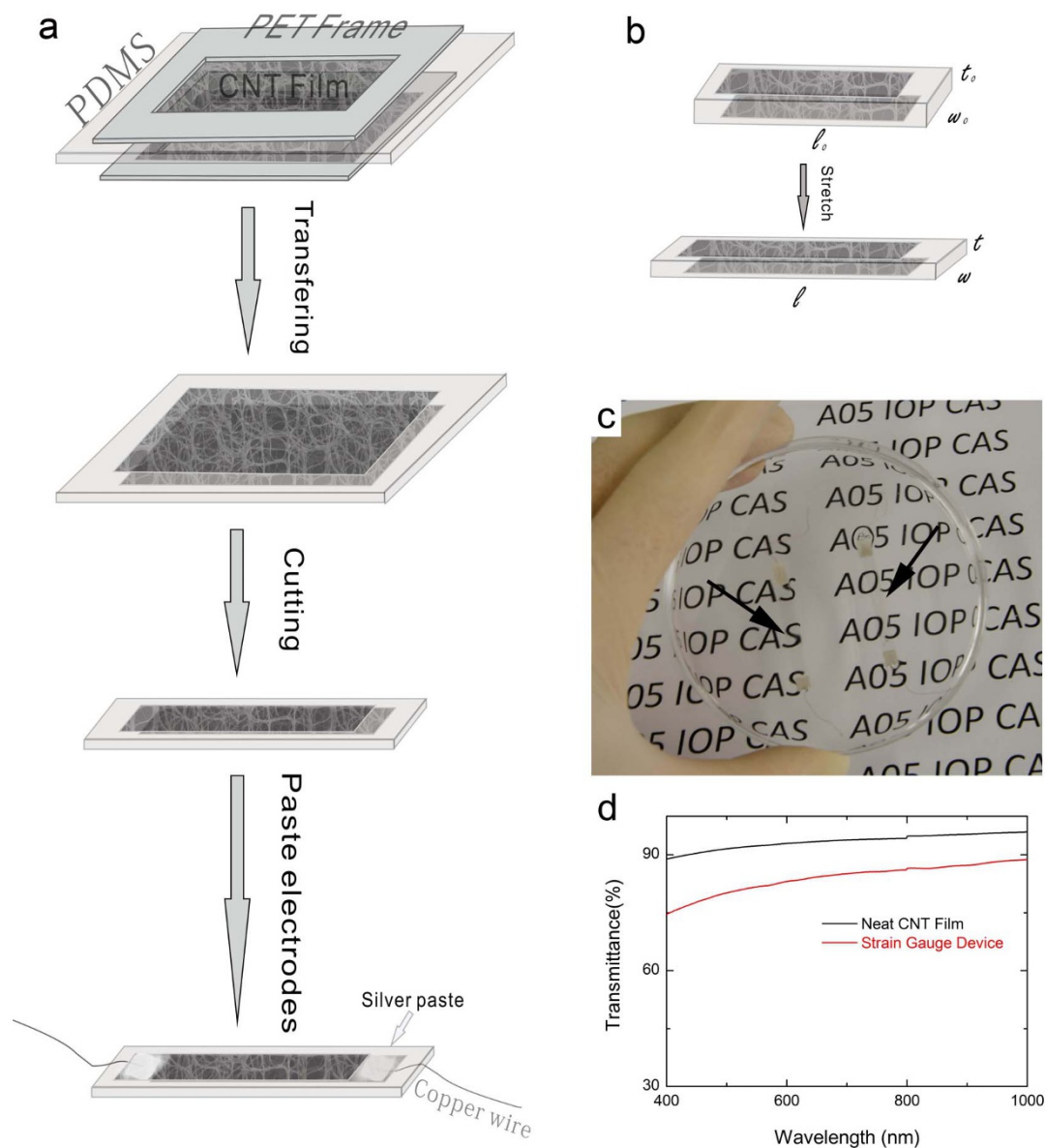
**Figure 1 | CNT-based transparent capacitive strain gauge.** (a) Schematic procedures of the fabrication of the strain gauges. (b) Operating mechanism of the Poisson strain gauge. (c) Optical picture of two as-prepared strain gauges in a petri dish. Arrows indicate the locations of the devices. (d) Transmittance spectra comparison of the neat CNT films and the corresponding CNT-based strain gauge in the wavelength range of 400–1000 nm.

translucent, excellent transparency could be acquired when the thickness was less than 1 mm.

**Stretchability of the composite electrodes.** The stretchability of the CNT/PDMS electrodes is crucial for the sensing performance of the final devices. Therefore, prior to capacitive response characterization, we investigated the resistance changes of the composite films under progressively increasing strains. As shown in Fig. 2d, strain-history dependence behaviors, featured by resistance plateaus, were observed[7,30]. The resistance kept unchanged in a certain strain range defined by the maximum strain ever applied. The sample remained conductive until mechanical failure over 140% strain, near the fracture strain of PDMS. To highlight the role of silicone matrix, we conducted in situ SEM characterizations on both neat CNT films and CNT/PDMS composite films (See Supplementary Fig. S1). The resistance of neat films rose steeply when the applied strain exceeded $\sim$ 15%, as a result of the ubiquitous gaps with sizes up to around 100 μm which were initiated by the stress concentration at weak points in the pristine films. CNT/PDMS composite films, in

contrast, showed relatively moderate increase in resistance and only occasional, several-micrometer-sized gaps even under strains as high as 100%. The silicone matrix evidently mitigated the concentration of stress, not only maintaining the structural integrity but also relieving the resistance increase of the composite films, both of which were beneficial for improving the strain gauging performances of the final devices. Thanks to the superior stretchability of the composite electrodes, the resulting strain gauges show excellent capacitive characters under a strain of 100% and excitation AC frequencies up to 200 kHz (see Supplementary Fig. S2). Nevertheless, the viscoelastic signatures, i.e. clear hysteresis and drift-over-time, deteriorated the resistive strain sensing capability of CNT/PDMS composite[30]. As to the presented CNT-based capacitive strain gauges, we will show below, the capacitance changes are absolutely stable, predictable and deterministic.

**Strain gauging performances.** We have to mention that the raw experimental data deviated from the predicted linear behavior once the applied strain exceeded 100%, which was attributed to the
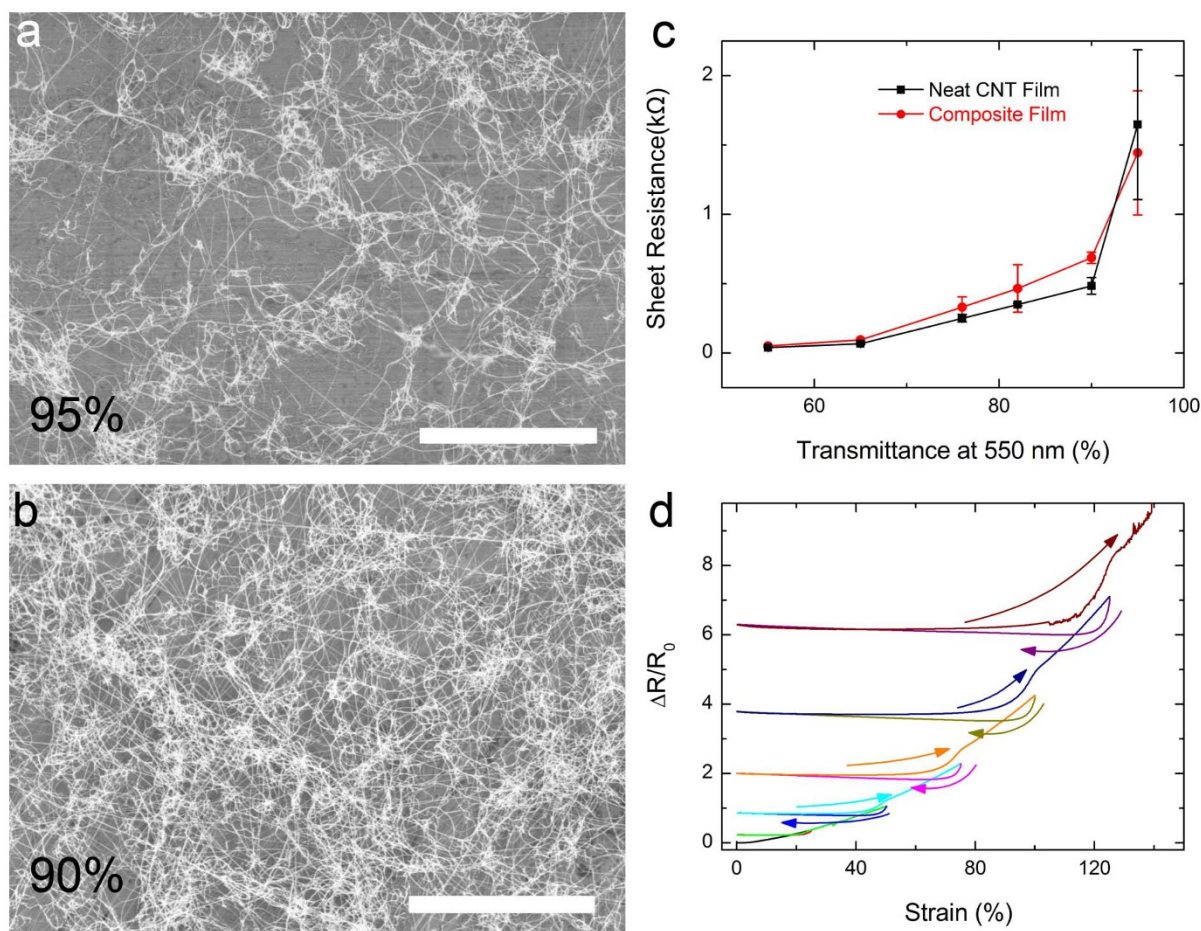
Figure 2 | **Morphological and electrical characterizations of the CNT-based electrodes.** (a–b) SEM images of continuously grown CNT films with transmittance of 95% (a) and 90% (b) at 550 nm. Scale bars, 5 μm. (c) Sheet resistance of neat CNT films and CNT/PDMS composite films with different optical transmittance. (d) Relative changes in resistance of a CNT/PDMS composite film under progressively increasing strains.

influence of the clamps. We adopted a special data treatment procedure to obtain the exact capacitive responses of the undisturbed strain gauges (see Supplementary Fig. S3 and Supplementary Note).

A strain gauge made from CNT/Dragon skin was subjected to a test with a complicated strain profile where the strain targets were progressively increased from 1% to 300%. A typical capacitive response curve was shown in Fig. 3a. In contrast to the resistance changes of the electrodes under a similar strain test (Fig. 2d), the capacitive response does not depend on the strain history, indicating reliable and deterministic performances of the CNT-based capacitive strain gauges. Besides, the triangle and trapezoid strain features were captured with high fidelity even at a strain as low as 1% (inset of Fig. 3a), implying that the smallest strain which was detectable should be well below 1%.

Figure 3b presents the capacitive responses of a sample device made from CNT/PDMS elastomer, in both stretching and releasing phases during a ramp process with a maximum strain of 100% and a speed of 5%/s. The simple linear model fit the experimental data perfectly ($R^2 \sim 0.9999$) with a slope of 0.97. Notably, no hysteresis was observed between the loading and unloading phase, highlighting the deterministic feature of the capacitive sensors. In addition, comparably excellent performance was obtained in the case of sensors made from CNT/Dragon skin elastomer in a much wider strain range of 0–300%, sufficient for most applications (See Supplementary Fig. S3 and S4). Furthermore, the gauge factor of our device is very close to the predicted value and represents the highest gauge factor of any strain gauge capable of detecting strains larger than 200%.

Long time durability is essential for practical applications because the devices will probably be exposed to long term and frequent use. We investigated the endurance of our strain gauges under repeated loading-unloading tests where the samples were cycled between valley (zero for all tests) and peak strains (100%, 150% and 200% in three parallel tests) with a sawtooth wave profile at a speed of 10 mm/s. Every thousand cycles, a "step-and-hold" test was taken where the sample was stretched to the maximum strains at a speed of 5 mm/s and held for 10 seconds before the strains were removed. Figure 3c shows the relative changes in capacitance, at both valley and peak strains, versus number of cycles. In all cases, the capacitance was very stable over the courses of cyclic stretching tests until the samples' catastrophic ruptures. The slow upward drift observed in the test with 150% strain was attributed to the poor fixing at the clamps, for the valley and peak capacitance drifted in tune. Figure 3d presents the curves of the first and the subsequent "step-and-hold" tests. For clarity, the curves with peak strains of 100% and 150% were offset along the horizontal axis. The baselines (the first "step-and-hold" test) and subsequent curves overlap each other, indicating excellent stability and reliability of our strain gauges. The tests with peak strains of 100%, 150% and 200% ended by structural failures at around the 10,000th, 3,800th and 1,800th cycle, respectively. It should be noted that the fracture initiated at the clamping points for all samples, implying that better endurance could be achieved by optimized structural or geometric designs. The only stretchable strain gauge that showed comparable durability with our device was reported by Yamada and coworkers (10,000 cycles at both 100% and 150% strains)[8].
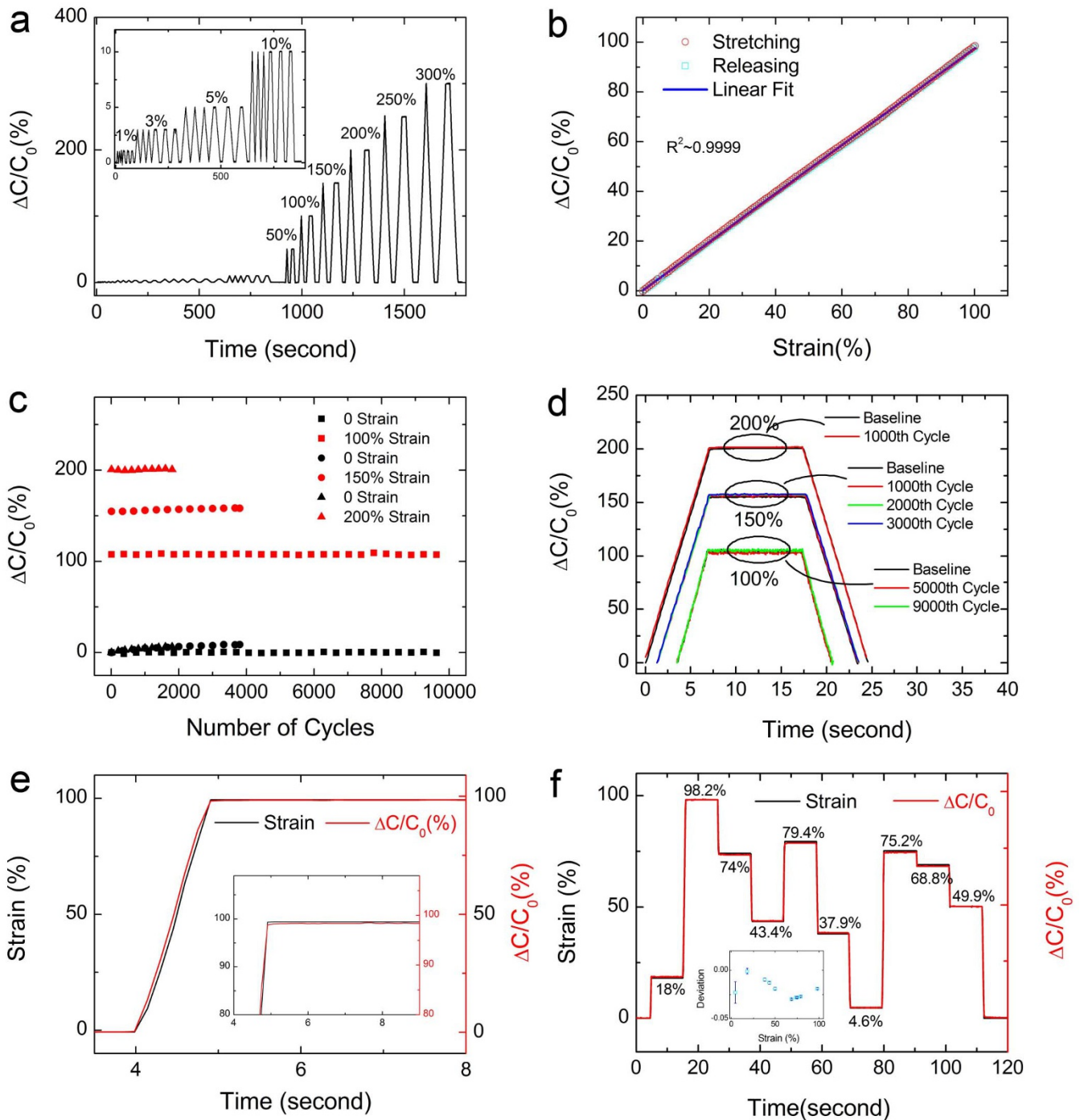
**Figure 3 | Systematic strain tests on the CNT-based capacitive strain gauge devices.** (a) Relative changes in capacitance of a strain gauge made from CNT/Dragon skin, under progressively increasing strains from 1% to 300%. (b) Capacitive response of a strain gauge made from CNT/PDMS during both loading (red circles) and unloading (green squares) of a strain of 100%, as well as the linear fit (blue line). (c–d) **Results of durability tests:** (c) Valley and peak values of capacitance versus number of cycles; (d) Curves of step-and-hold tests for the labeled peak strains and cycles. (e) Capacitive response (red) to fast step-and-hold strains (black, precisely measured using a laser motion monitor). Inset: Close-up of the overshoot. (f) Relative changes in capacitance (red) in response to a series of random values of strain (black, precisely measured using a laser motion monitor). Inset: Average normalized deviations between the measured strains and capacitive response.

Most CNT based resistive strain gauges show poor dynamic response featured by obvious overshoots and relaxation, due to the viscoelasticity of polymer matrix and ubiquitous frictions between CNTs and polymer molecules. We investigated the dynamic response of our device by cycling the sample between 0 and 100% strain at a speed of 20 mm/s, with a recovery time of 10 seconds at each stage. The capacitive response is almost instantaneous with a delay time well beyond the resolution of our instruments (~100 ms), as

shown in Fig. 3e. Furthermore, no noticeable overshoot or relaxation was observed, as can be seen in the inset of Fig. 3e. These results were impressive, since the resistance changes of the composite electrodes suffered from severe overshoots and relaxation. Despite the viscoelasticity of silicone elastomer and frictions between CNTs and polymer molecules, the capacitive response of our strain gauges is very fast, stable and deterministic, making them suitable for applications where dynamic loading is involved. The sample was further subjected

to a series of random strains, the values of which were generated by a random number generator, at a speed of 20 mm/s and with a holding time of 10 seconds, as shown in Fig. 3f. The capacitance changes were found to well match the strain values measured by the laser motion monitor, with the average normalized deviations on the order of $10^{-2}$ (inset).

To the best of our knowledge, this is the first report of uniaxial strain gauges that can detect strains up to 300% with resolution < 1%, own superior optical transparency, durability and fast response, and are free of hysteresis and creep. In addition, our strain sensors exhibit excellent linearity throughout the whole strain range, which is beneficial for many practical applications. Furthermore, our devices are monolithic and the polymer coating can protect the CNT electrodes from humidity and chemical species that might affect the electronic properties of carbon nanotubes. However, temperature variation might affect the capacitive response due to thermal expansion and contraction. We measured the capacitance of a strain gauge while the environment temperature rose from 20°C to 100°C and found a temperature sensitivity of −0.13%/°C (See Supplementary Fig. S5), in agreement with the calculation of Cohen et al[17]. This small temperature coefficient indicates that our strain gauges, unlike traditional piezoresistors, are essentially invulnerable to temperature changes. Besides, temperature variations are often characterized by slow drifts and can be compensated by a thermometer.

**Human motion detection.** The technological goal is to integrate such sensors onto smart clothes or directly onto the body to monitor human motions in real time (see Fig. 4 and Supplementary Movie S1), which might find applications in rehabilitation, virtual reality and health monitoring. We demonstrated a prototypical data glove by integrating a strain gauge onto a rubber glove to detect the bending movements of the fingers. Unlike optical fibers and metal foil strain gauges that are widely adopted as the sensing elements in cyber gloves[42], our stretchable strain gauges allow easy and multiple integration and do not constrain the motions of hands. When the demonstrator's fingers were gradually folded, the capacitance of the sensor increased step by step (stage I to V, Fig. 4a), distinguishing every single slight bending. The capacitance returned to the initial value once the fingers were completely unfolded (stage VI to VIII, Fig. 4a). Notably, when the finger was kept at a certain angle, the sensor's capacitance remained constant, thanks to the excellent stability and reliability of the capacitive strain gauge. The unexpected sharp peaks, e.g. the one marked by the arrow, arose from an accidental disruption of the copper wire electrodes. Replacing silver paste with liquid metal, e.g. Galinstan[7], or stretchable CNT conductive paste can be a good solution[4,8]. The use of this kind of sensors in various areas might benefit both daily and engineering activities. For example, the sensors might help to remotely control slave robots in doing delicate or dangerous work that may be out of reach for human body.
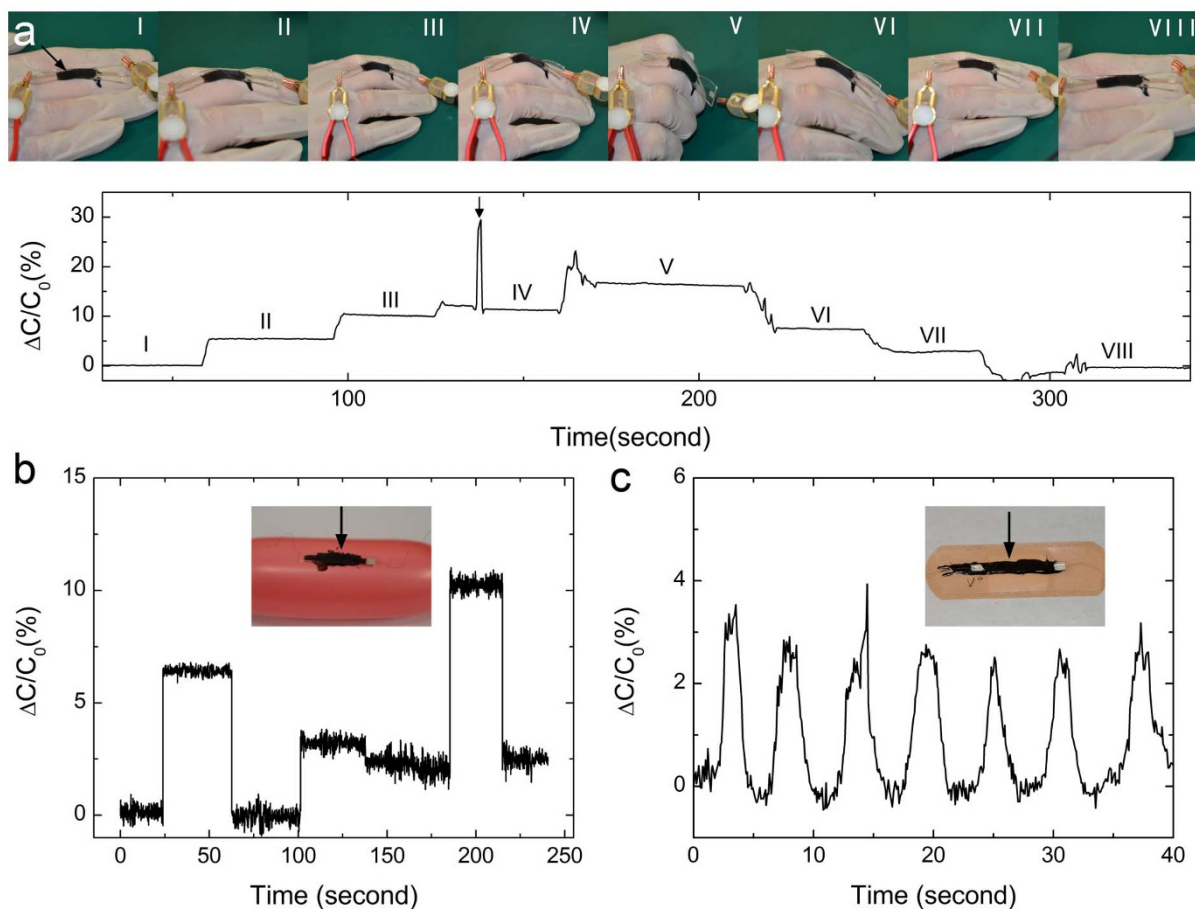


**Figure 4 | Demonstrations of using the strain gauges to detect human motion.** (a) A prototypical data glove. Upper: Still pictures while the finger was gradually folded (I–V) and then unfolded (VI–VIII). Lower: Corresponding capacitive responses. Arrow: An accidental disrupt of the copper wire. (b) Capacitive changes of a strain gauge bonded onto a balloon in response to the inflation and deflation of the balloon. Inset: Optical picture of the strain gauge bonded onto a balloon. (c) Capacitive changes of a device integrated with a bandage responding to the movements of human chest while breathing. Inset: Optical picture of the strain gauge bonded onto a bandage. **Note:** The strain gauges (indicated by arrows) appear black and non-uniform because the RTV silicone rubber used to bond them was black.

In another demonstration, a strain gauge was assembled with a balloon (Fig. 4b) to measure the strains associated with the inflation and deflation of the balloon, resembling the movements of human chest while inhaling and exhaling. Unambiguous capacitance rises and drops occurred when the balloon expanded or shrank, as shown in Fig. 4b. In order to manifest the applicability of such a device, we bonded a device onto a bandage, and used it to monitor the movements of human chest while breathing. The device exhibited distinct response to every heave of the chest (Fig. 4c). The profile of the capacitive response curves—slopes, frequency and amplitudes—reflects that of human respiration. In addition, spatial resolution can be achieved by integrating several strain gauges at multiple locations and along different directions. Such devices can be used as human health monitors, such as the construction of early warning system for sudden infant death syndrome (SIDS)[43].

## Discussion

We designed and fabricated a new transparent and stretchable CNT-based capacitive strain gauge that could detect strains from below 1% to 300% with excellent linearity and high sensitivity. Systematic and elaborate strain tests confirmed superior stability, durability and reliability of the devices. A combination of outstanding strain gauging performances, optical transparency, physical robustness and easy fabrication may promise potentially wide applications in bio-interactive and intelligent electronics, as exemplified by the prototypical data glove and respiration monitor. In addition, large scale production and patterning can be realized by applying roll-to-roll assembling, stencil masking and laser cutting strategies. Furthermore, the sensitivity of the strain gauge can be further improved through optimizing the device structures or tailoring the properties of dielectric medium, e.g. adopting an anisotropic elastomer with different in-plane and out-of-plane Poisson ratios. Therefore, our investigations represent an inspiring achievement in overcoming the drawbacks of conventional sensors and may provide a new way to construct new-generation multifunctional wearable and implantable electronics for plenty of applications.

## Methods

**Synthesize of CNT films.** Carbon nanotube films were continuously grown through a floating catalyst vapor deposition (FCCVD) method similar to that of Windle et al[41]. The sheet resistance and optical transmittance could be controlled by adjusting the growth conditions. The films were collected onto PET frames with rectangular hollows of the desired sizes.

**Preparation of silicone lamina.** For the PDMS lamina, silicone oligomer (Dow Corning, Sylgard 184 silicone elastomer kit) was mixed with cross-linker (weight ratio 10 : 1), stirred for 20 minutes, degassed, poured into a petri dish and cured at 70°C for 2 hours. For the Dragon skin (Smooth-on, Dragon skin 30 trial size) film, similar procedure was applied, whereas the weight ratio of part A to part B was 1 : 1 and the curing conditions were 70°C and 4 hours. The thickness of the silicone films was controlled to be below 0.5 mm.

**Fabrication of capacitive strain gauge.** PET frames bearing CNT films were brought into contact with the PDMS lamina and the CNT films were transferred onto the surface of PDMS. The stickiness of PDMS and high surface energy of carbon nanotubes ensured good adhesion between PDMS and CNT films. An overlap length of at least 10 mm was ensured between the CNT films on the two sides of PDMS. Then, the CNT/silicone/CNT was cut into strips of 2 mm wide. Copper wires were connected to the opposing CNT films at the two ends using silver paste. Finally, the whole device was immersed into liquid PDMS so that molecular coupling was formed between the nanotubes and PDMS molecules. For the demonstration of human motion detection, a strain gauge was integrated onto the targets, i.e. the rubber glove, balloon and bandage, using room-temperature-vulcanized (RTV) rubber paste. The electrodes were left free so as not to be disturbed by the strains of the targets. All the experiments that were conducted on human fingers and chest were performed under guidelines and regulations. No other human subjects were involved in our experiments or manuscript.

**Cyclic strain tests.** Tensile strains were loaded and unloaded using a laboratory-made stretching stage equipped with a stepper motor and controlled by the computer. The stage consisted of an actuating unit (moving part) and a stationary part. Before stretching operation, the sample was clamped onto the stage with the stretching part of about 10 mm in length, leaving the copper wires outside the stretching part.

**Characterization methods.** Resistance of the CNT films and composite films was measured using a Keithley 2400 multimeter. Capacitance of the devices was measured by a NF ZM2353 LCR meter, whereas a capacitive Wheatstone bridge can serve as a more convenient and portable alternative. An excitation frequency of 5 kHz was chosen to ensure both good signal-to-noise level and capacitive characteristics. The displacement of the actuating unit, thus the strain of the sample, was precisely monitored using a laser displacement sensing system (Keyence, LK G5001V and LK-H050). All the above equipment was controlled by the computer through a LabView program. All the mechanical-electrical characterizations, unless specially stated, were conducted at ambient environment. Microscopic morphology was characterized using a scanning electron microscopy (SEM) system (HiTachi FESEM 4800). Optical transmittance spectra were recorded by a UV-vis-NIR spectrometer (Varian Cary 5000).

**In situ SEM characterizationunder tensile strains.** In order to avoid the complete failure of CNT films when subjected to large strains, neat films were laid onto cured PDMS and flattened with ethanol to ensure good adhesion between the CNT films and PDMS substrates. The composite films where CNTs were embedded in PDMS matrix were not suitable for in situ morphological characterization because of the thick coating of insulating polymer. Therefore, special consideration was necessary to make CNTs visible under electron beams. We firstly flattened a piece of CNT film in a petri dish, then poured liquid PDMS onto the film and cured. In this way, CNTs was inlaid into just the top surface of PDMS and allowed to be seen under electron beam. In fact, an ultrathin composite layer was formed because the voids of CNT film was penetrated and filled with PDMS molecules. In situ SEM characterization was conducted where the sample was mounted onto a specially designed stretching stage that fit the size of the chamber of the SEM.

**Temperature coefficient estimation.** We assessed the temperature stability of a strain gauge device by measuring the capacitance under controlled environment temperature, which rose from 20°C to 100°C at step of 10°C. A stabilization time of 1 hour was held for each value of temperature.

1. Kim, D.-H., Xiao, J., Song, J., Huang, Y. & Rogers, J. A. Stretchable, Curvilinear Electronics Based on Inorganic Materials. *Adv. Mater.* **22**, 2108–2124 (2010).
2. Sekitani, T. & Someya, T. Stretchable, Large-area Organic Electronics. *Adv. Mater.* **22**, 2228–2246 (2010).
3. Rogers, J. A., Someya, T. & Huang, Y. Materials and Mechanics for Stretchable Electronics. *Science* **327**, 1603–1607 (2010).
4. Sekitani, T. *et al.* Stretchable active-matrix organic light-emitting diode display using printable elastic conductors. *Nat. Mater.* **8**, 494–499 (2009).
5. Ko, H. C. *et al.* A hemispherical electronic eye camera based on compressible silicon optoelectronics. *Nature* **454**, 748–753 (2008).
6. Kim, D.-H. *et al.* Epidermal Electronics. *Science* **333**, 838–843 (2011).
7. Lipomi, D. J. *et al.* Skin-like pressure and strain sensors based on transparent elastic films of carbon nanotubes. *Nat. Nanotechnol.* **6**, 788–792 (2011).
8. Yamada, T. *et al.* A stretchable carbon nanotube strain sensor for human-motion detection. *Nat. Nanotechnol.* **6**, 296–301 (2011).
9. Pang, C. *et al.* A flexible and highly sensitive strain-gauge sensor using reversible interlocking of nanofibres. *Nat. Mater.* **11**, 795–801 (2012).
10. Mannsfeld, S. C. B. *et al.* Highly sensitive flexible pressure sensors with microstructured rubber dielectric layers. *Nat. Mater.* **9**, 859–864 (2010).
11. McAlpine, M. C., Ahmad, H., Wang, D. & Heath, J. R. Highly ordered nanowire arrays on plastic substrates for ultrasensitive flexible chemical sensors. *Nat. Mater.* **6**, 379–384 (2007).
12. Takei, K. *et al.* Nanowire active-matrix circuitry for low-voltage macroscale artificial skin. *Nat. Mater.* **9**, 821–826 (2010).
13. Munro, B. J., Campbell, T. E., Wallace, G. G. & Steele, J. R. The intelligent knee sleeve: A wearable biofeedback device. *Sensor Actuat. B-chem* **131**, 541–547 (2008).
14. Kang, I., Schulz, M. J., Kim, J. H., Shanov, V. & Shi, D. A carbon nanotube strain sensor for structural health monitoring. *Smart Mater. Struct.* **15**, 737–748 (2006).
15. Mattmann, C., Clemens, F. & Troester, G. Sensor for measuring strain in textile. *Sensors* **8**, 3719–3732 (2008).
16. Ilievski, F., Mazzeo, A. D., Shepherd, R. E., Chen, X. & Whitesides, G. M. Soft Robotics for Chemists. *Angew. Chem. Int. Edit.* **50**, 1890–1895 (2011).
17. Cohen, D. J., Mitra, D., Peterson, K. & Maharbiz, M. M. A Highly Elastic, Capacitive Strain Gauge Based on Percolating Nanotube Networks. *Nano Lett.* **12**, 1821–1825 (2012).
18. Gamble, J., Gartside, I. B. & Christ, F. A reassessment of mercury in silastic strain-gauge plethysmography for microvascular permeability assessment in man. *J. Physiol-london.* **464**, 407–422 (1993).
19. Khang, D. Y., Jiang, H. Q., Huang, Y. & Rogers, J. A. A stretchable form of single-crystal silicon for high-performance electronics on rubber substrates. *Science* **311**, 208–212 (2006).
20. Sekitani, T. *et al.* A rubberlike stretchable active matrix using elastic conductors. *Science* **321**, 1468–1472 (2008).
21. Chun, K.-Y. *et al.* Highly conductive, printable and stretchable composite films of carbon nanotubes and silver. *Nat. Nanotechnol.* **5**, 853–857 (2010).
22. Kim, K. S. *et al.* Large-scale pattern growth of graphene films for stretchable transparent electrodes. *Nature* **457**, 706–710 (2009).

23. Lacour, S. P., Wagner, S., Huang, Z. Y. & Suo, Z. Stretchable gold conductors on elastomeric substrates. *Appl. Phys. Lett.* **82**, 2404–2406 (2003).

24. Park, M. *et al.* Highly stretchable electric circuits from a composite material of silver nanoparticles and elastomeric fibres. *Nat. Nanotechnol.* **7**, 803–809 (2012).

25. De Volder, M. F. L., Tawfick, S. H., Baughman, R. H. & Hart, A. J. Carbon Nanotubes: Present and Future Commercial Applications. *Science* **339**, 535–539 (2013).

26. Liu, L., Ma, W. & Zhang, Z. Macroscopic Carbon Nanotube Assemblies: Preparation, Properties, and Potential Applications. *Small* **7**, 1504–1520 (2011).

27. Foroughi, J. *et al.* Torsional Carbon Nanotube Artificial Muscles. *Science* **334**, 494–497 (2011).

28. Ma, W. *et al.* High-Strength Composite Fibers: Realizing True Potential of Carbon Nanotubes in Polymer Matrix through Continuous Reticulate Architecture and Molecular Level Couplings. *Nano Lett.* **9**, 2855–2861 (2009).

29. Li, J. *et al.* Superfast-Response and Ultrahigh-Power-Density Electromechanical Actuators Based on Hierarchal Carbon Nanotube Electrodes and Chitosan. *Nano Lett.* **11**, 4636–4641 (2011).

30. Cai, L. *et al.* Highly Transparent and Conductive Stretchable Conductors Based on Hierarchical Reticulate Single-Walled Carbon Nanotube Architecture. *Adv. Funct. Mater.* **22**, 5238–5244 (2012).

31. Hecht, D. S. *et al.* High conductivity transparent carbon nanotube films deposited from superacid. *Nanotechnology* **22**, 075201 (2011).

32. Liu, K. *et al.* Cross-Stacked Superaligned Carbon Nanotube Films for Transparent and Stretchable Conductors. *Adv. Funct. Mater.* **21**, 2721–2728 (2011).

33. Zhang, Y. Y. *et al.* Polymer-Embedded Carbon Nanotube Ribbons for Stretchable Conductors. *Adv. Mater.* **22**, 3027–3031 (2010).

34. Shin, M. K. *et al.* Elastomeric Conductive Composites Based on Carbon Nanotube Forests. *Adv. Mater.* **22**, 2663–2667 (2010).

35. Xu, F., Wang, X., Zhu, Y. T. & Zhu, Y. Wavy Ribbons of Carbon Nanotubes for Stretchable Conductors. *Adv. Funct. Mater.* **22**, 1279–1283 (2012).

36. Yu, Z., Niu, X., Liu, Z. & Pei, Q. Intrinsically Stretchable Polymer Light-Emitting Devices Using Carbon Nanotube-Polymer Composite Electrodes. *Adv. Mater.* **23**, 3989–3994 (2011).

37. Niu, Z. *et al.* Highly Stretchable, Integrated Supercapacitors Based on Single-Walled Carbon Nanotube Films with Continuous Reticulate Architecture. *Adv. Mater.* **25**, 1058–1064 (2013).

38. Xiao, L. *et al.* Flexible, Stretchable, Transparent Carbon Nanotube Thin Film Loudspeakers. *Nano Lett.* **8**, 4539–4545 (2008).

39. Jung, Y. J. *et al.* Aligned carbon nanotube-polymer hybrid architectures for diverse flexible electronic applications. *Nano Lett.* **6**, 413–418 (2006).

40. Palmer, H. B. The Capacitance of a Parallel-Plate Capacitor by the Schwartz-Christoffel Transformation. *Trans. Am. Inst. Electr. Eng.* **56**, 363–366 (1937).

41. Li, Y. L., Kinloch, I. A. & Windle, A. H. Direct spinning of carbon nanotube fibers from chemical vapor deposition synthesis. *Science* **304**, 276–278 (2004).

42. Hanly, E. J. & Talamini, M. A. Robotic abdominal surgery. *Am. J. Surg.* **188**, 19S–26S (2004).

43. Fleming, P. J. *et al.* Interaction Between Bedding and Sleeping Position In the Sudden-infant-death-syndrome - A Population Based Case-control Study. *Brit. Med. J.* **301**, 85–89 (1990).

## Author contributions

L.C., L.S. and S.X. designed the experiments. L.C. performed the sample fabrication, strain tests and SEM characterizations. L.C., P.L., Q.G. and J.L. conducted the electrical measurements. Q.Z. and N.Z. performed the growth of CNT films. L.C., L.S., D.Z., X.Z., Q.Z., P.A. and S.X. discussed and wrote the manuscript. M.T., F.Y., W.Z., Q.F., W.Z. contributed to extensive discussion and the data analysis.

## Additional information

**Supplementary information** accompanies this paper at http://www.nature.com/scientificreports

**Competing financial interests:** The authors declare no competing financial interests.

**How to cite this article:** Cai, L. *et al.* Super-stretchable, Transparent Carbon Nanotube-Based Capacitive Strain Sensors for Human Motion Detection. *Sci. Rep.* **3**, 3048; DOI:10.1038/srep03048 (2013).

**CORRIGENDUM:** Super-stretchable, Transparent Carbon Nanotube-Based Capacitive Strain Sensors for Human Motion Detection

Le Cai, Li Song, Pingshan Luan, Qiang Zhang, Nan Zhang, Qingqing Gao, Duan Zhao, Xiao Zhang, Min Tu, Feng Yang, Wenbin Zhou, Qingxia Fan, Jun Luo, Weiya Zhou, Pulickel M. Ajayan & Sishen Xie